

# Polarization Rotation Correction in Radiometry: An Extended Error Analysis

Derek L. Hudson<sup>1</sup>, Jeffrey R. Piepmeier<sup>2</sup>, David G. Long<sup>1</sup>

<sup>1</sup>Brigham Young University, Provo, Utah USA 84602. Email: dlh8@et.byu.edu

<sup>2</sup>NASA's Goddard Space Flight Center, Greenbelt, Maryland, USA

**Abstract**—Yueh [1] proposed a method of using the third Stokes parameter,  $T_U$ , to correct brightness temperatures, such as  $T_v$  and  $T_h$ , for polarization rotation. This paper presents an extended error analysis of the retrieval of  $T_Q \equiv T_v - T_h$  by Yueh's method.

Analytical formulas are derived for the bias, standard deviation, and mean-squared error (MSE) of retrieved  $T_Q$ , as functions of scene and radiometer parameters. These formulas are validated through independent calculation via Monte Carlo simulation.

The formulas predict several interesting effects: (a) MSE is minimized by rotating the radiometer by  $45^\circ$  with respect to the natural polarization basis defined by the Earth's surface, (b)  $T_U$  from planetary surface radiation (of the magnitude expected on Earth) has a negligible effect on correction for polarization rotation, and (c) three-channel polarimetric radiometry (with the radiometer rotated by  $45^\circ$ ) has lower MSE than conventional two-channel radiometry that suffers no polarization rotation.

## I. INTRODUCTION

The earth's ionosphere and magnetic field cause Faraday rotation of the polarization of radiation emanating from the earth's surface. This rotation mixes the vertical and horizontal polarization components of brightness temperatures,  $T_v$  and  $T_h$ , degrading the measurement of both. For L-band satellite measurements at  $40^\circ$  incidence angle, resulting errors in the oft-used  $T_Q \equiv T_v - T_h$  can reach 4 to 12 K. Additional polarization rotation occurs if a sensor's antenna feed polarization basis is rotated with respect to the natural polarization basis of the earth's surface.

SMOS and Aquarius are being designed to measure polarization rotation (especially Faraday rotation) and correct for it in post-processing. The basic method involves measuring the third Stokes parameter,  $T_U$ , in addition to the usual  $T_v$  and  $T_h$ . The method is introduced by Yueh in [1].

When Yueh presented the technique, he also performed a first-order error analysis. This paper examines error in estimated  $T_Q$  in greater depth. We report the underlying model and the results, omitting many details for lack of space.

## II. FORWARD PROBLEM

Our most basic foundation is a model of the electric fields,

$$\begin{bmatrix} x(t) \\ y(t) \end{bmatrix} = \begin{bmatrix} \cos \Omega & \sin \Omega \\ -\sin \Omega & \cos \Omega \end{bmatrix} \begin{bmatrix} E_v(t) \\ E_h(t) \end{bmatrix} + \begin{bmatrix} a(t) \\ b(t) \end{bmatrix}. \quad (1)$$

(In the sequel, the dependences on  $t$  are suppressed.)  $E_v$  and  $E_h$  are the components of the total electric field emitted by the scene in the vertical and horizontal directions, respectively.

Because the number of independent emitters in the scene is large in spaceborne radiometry,  $E_v$  and  $E_h$  are normally distributed, by the central limit theorem, with zero means [2]. Their correlation defines the third Stokes parameter:  $Cov(E_v, E_h) = E(E_v E_h) - 0 \equiv T_U/2$  where  $E(\cdot)$  denotes the expected value. (In this and subsequent definitions, we ignore a proportionality constant which converts the product of two electric fields to a brightness temperature.)

$E_v$  and  $E_h$  are rotated through an angle  $\Omega$ . Receiver noise is then added, represented by the electric field amplitudes  $a$  and  $b$ . Like  $E_v$  and  $E_h$ , we assume that  $a$  and  $b$  are normally distributed, zero mean, normal random variables. We also assume they are independent of one another and of  $E_v$  and  $E_h$ . This model neglects sidelobe contributions (as they may undergo different amounts of rotation than the main beam radiation) and cross-coupling of the polarization components caused by the antenna and radiometer.

A quantity of high interest to users of radiometry data is the second Stokes parameter,  $T_Q \equiv T_v - T_h \equiv E(E_v^2) - E(E_h^2)$ . Three-channel polarimetric radiometers measure the three quantities

$$\hat{T}_{va} = \frac{1}{\tau} \int_0^\tau x^2 dt, \quad \hat{T}_{ha} = \frac{1}{\tau} \int_0^\tau y^2 dt, \quad \hat{T}_{Ua} = \frac{2}{\tau} \int_0^\tau xy dt. \quad (2)$$

As shown in [2], these can be rewritten as sums of independent samples,

$$\hat{T}_{va} = \frac{1}{N} \sum_{i=1}^N x_i^2, \quad \hat{T}_{ha} = \frac{1}{N} \sum_{i=1}^N y_i^2, \quad \hat{T}_{Ua} = \frac{2}{N} \sum_{i=1}^N x_i y_i, \quad (3)$$

where  $N = 2 * \text{sensor bandwidth} * \text{integration time} \equiv 2B\tau$ . In this paper we are concerned only with  $\hat{T}_{Ua}$  and  $\hat{T}_{Qa} \equiv \hat{T}_{va} - \hat{T}_{ha}$ .

Under the assumption that  $\hat{T}_{Ua}$  and  $\hat{T}_{Qa}$  are Gaussian (which is a very good approximation because  $N$  is very large), and using (1), we are able to show that

$$\hat{T}_{Qa} = T_Q \cos 2\Omega + T_U \sin 2\Omega + T_{RX,Q} + \Delta T_{Qa} \quad (4)$$

$$\hat{T}_{Ua} = -T_Q \sin 2\Omega + T_U \cos 2\Omega + \Delta T_{Ua} \quad (5)$$

where  $T_{RX,Q} \equiv E(a^2) - E(b^2)$  and where  $\Delta T_{Qa}$  and  $\Delta T_{Ua}$  are normally distributed with zero means, known variances, and known, nonzero covariance.

$T_{RX,Q}$  is operationally estimated and subtracted off as part of the radiometer data calibration. Imperfection in this

correction leaves a residual which we call  $\Delta T_{RX,Q}$ , so a revised forward model of the  $\hat{T}_{Qa}$  measurement is

$$\hat{T}'_{Qa} = T_Q \cos 2\Omega + T_U \sin 2\Omega + \Delta T_{RX,Q} + \Delta T_{Qa}. \quad (6)$$

### III. ESTIMATION OF $T_Q$ BY YUEH'S METHOD

Yueh's model [1] does not include any of the  $\Delta$  terms in (5) and (6). By noting that  $T_U$  is much smaller than  $T_Q$  in natural earth scenes, he proposes to solve (5) and (6) for  $T_Q$  by neglecting the terms with  $T_U$ , squaring both sides of (5) and (6), adding the two results, and then solving for  $T_Q$ . This yields

$$\hat{T}_Q = \sqrt{\hat{T}'_{Qa}{}^2 + \hat{T}'_{Ua}{}^2}. \quad (7)$$

### IV. ERROR ANALYSIS OF $\hat{T}_Q$

#### A. Analytical derivation/results

We wish to find analytical formulas for the mean and variance of (7), given the model developed above.  $\hat{T}'_{Qa}$  and  $\hat{T}'_{Ua}$  are correlated, but an appropriate rotation forms the uncorrelated variables  $Z$  and  $W$ , and  $\hat{T}_Q = \sqrt{Z^2 + W^2}$ .  $Z$  and  $W$  have known (albeit somewhat complicated) means and variances in terms of  $T_Q, T_U, \Omega, T_{RX,Q}, \Delta T_{RX,Q}, T_I \equiv T_v + T_h$ , and  $T_{RX,I} \equiv E(a^2) + E(b^2)$ . If we employ the minor approximation that the variances of  $Z$  and  $W$  are equal, the pdf of  $\hat{T}_Q$  is simple [3] and the mean and variance are also known [4], reducing to

$$E(\hat{T}_Q) = \sigma \sqrt{\frac{\pi}{2}} {}_1F_1\left(-\frac{1}{2}, 1; -\frac{m^2}{2\sigma^2}\right) \quad (8)$$

$$Var(\hat{T}_Q) = 2\sigma^2 + m^2 - [E(\hat{T}_Q)]^2 \quad (9)$$

where  ${}_1F_1$  is the confluent hypergeometric function and

$$\sigma^2 \equiv \frac{(T_I + T_{RX,I})^2}{N} \quad (10)$$

$$m^2 \equiv T_Q^2 + T_U^2 + \Delta T_{RX,Q}^2 + 2\Delta T_{RX,Q}(T_Q \cos 2\Omega + T_U \sin 2\Omega). \quad (11)$$

At least for the range of  $\sigma^2$  and  $m^2$  in which we have interest, we find that (8) and (9) are very well approximated by

$$E(\hat{T}_Q) \approx \sqrt{\sigma^2 + m^2} \quad (12)$$

$$Var(\hat{T}_Q) \approx \sigma^2. \quad (13)$$

Mean squared error (MSE) is a better way to measure the merit of an estimator than bias ( $\equiv E(\hat{T}_Q) - T_Q$ ) or standard deviation ( $STD \equiv \sqrt{Var}$ ) alone because it is a direct measure of the error in the estimate. It is a combination of bias and STD, in fact the sum of their squares, that is

$$\begin{aligned} MSE(\hat{T}_Q) &\equiv E\left([\hat{T}_Q - T_Q]^2\right) = bias^2 + STD^2 \\ &\approx 2\sigma^2 + m^2 + T_Q^2 - 2T_Q\sqrt{\sigma^2 + m^2}. \end{aligned} \quad (14)$$

#### B. Comparison with Monte Carlo results

The mean and variance of  $\hat{T}_Q$  can also be found by Monte Carlo simulation. This can be done using (1) and (3) directly, thus avoiding the subsequent approximations used to derive (12), (13), and (14).

The precise procedure is to generate  $N$  samples of  $a, b, E_v$ , and  $E_h$ , all independent of one another except  $E(E_v E_h) = T_U/2$ . From these,  $N$  samples of  $x$  and  $y$  are formed according to (1) and then squared and averaged to produce a single sample of  $\hat{T}'_{Qa}$  and  $\hat{T}'_{Ua}$  as in (3). These are used in (7) to form a single sample of  $\hat{T}_Q$ . This entire procedure is repeated  $M$  times to form  $M$  independent samples of  $\hat{T}_Q$ . The empirical mean and variance of  $\hat{T}_Q$  can then be calculated from these samples, and they converge to the true mean and variance as  $M$  increases.

These Monte Carlo results are compared with the predictions of (12), (13), and (14) in the figures below, for some of the most extreme values of the parameters that are expected in two cases. Fig. 2 is for a very long integration time (12 s) and other parameters of NASA's Aquarius mission (for the beam with smallest incidence angle,  $\theta = 23.3^\circ$ ). Fig. 2 is the same but for  $\theta = 41.7^\circ$ . Fig. 3 is for a much shorter integration time (0.016 s),  $\theta = 41.7^\circ$ , and other parameters that have been proposed for sensing soil moisture at L-band. (The bias in Fig. 2 is approximately the negative of the bias in the other two figures because we used the opposite sign for  $\Delta T_{RX,Q}$ .) Monte Carlo simulations have also been performed for many other values of  $T_Q, T_U, \Delta T_{RX,Q}, \Omega$ , and  $N$ . The results are in very close agreement with (12), (13), and (14) in all cases, thus validating those formulas.

#### C. Insights

These results lead us to the following conclusions:

1) MSE is a function of  $\Omega$  when  $\Delta T_{RX,Q} \neq 0$ . It can be reduced by minimizing  $\Delta T_{RX,Q}$  and/or by operating near  $\Omega = 45^\circ$ , which can be done by deliberately rotating the sensor by  $45^\circ$  with respect to the natural polarization basis of the scene.

2)  $T_U$  is not a significant error source in polarization rotation correction, at least at L-band. Its only effect is through  $m$ . From (11) we see that its effects run parallel to those of  $T_Q$ . Because  $T_Q$  is so much larger than  $T_U$  (at least at L-band and for natural earth scenes), the effect of  $T_U$  is somewhat negligible. Nonzero  $T_U$  does cause the peaks in bias and MSE to be larger at  $\Omega = \pm 90^\circ$  than at  $\Omega = 0^\circ, 180^\circ$ . This effect is largest for small incidence angles, since this makes  $T_Q$  smaller.

3) Superiority over conventional radiometry: in conventional two-channel radiometry,  $\hat{T}'_{Ua}$  is not measured and  $\Omega$  originating from the ionosphere is small enough at high frequencies that it can be neglected. Under these circumstances, we have, from (7) and (6),  $\hat{T}_Q = \hat{T}'_{Qa} = T_Q + \Delta T_{RX,Q} + \Delta T_{Qa}$ . If  $\Delta T_{RX,Q}$  is slowly varying then  $\hat{T}_Q$  has a bias of  $\Delta T_{RX,Q}$  and a variance equal to the variance of  $\Delta T_{Qa}$ . This variance has been derived analytically using the same assumptions that gave (6). At  $\Omega = 0$  it reduces to  $\sigma^2 + [(T_Q + T_{RX,Q})^2 - T_U^2]/N$ .

The bias, STD, and MSE from these expressions are plotted as asterisks in the figures, at  $\Omega = 0$ . From these and from similar plots using the analytic formulas, we see that three-channel polarimetric radiometry, operated near  $\Omega = 45^\circ$ , outperforms (in terms of MSE) conventional two-channel radiometry operating near  $\Omega = 0^\circ$ . In fact, the advantage of three-channel radiometry is approximately  $(\Delta T_{RX,Q})^2$  in MSE, whose square root is  $|\Delta T_{RX,Q}|$  K. (One exception: in the Aquarius case, 2-channel radiometry can be slightly superior (at most 0.0015 in MSE, whose square root is 0.04 K) when  $|\Delta T_{RX,Q}|$  is very small, e.g. less than 0.04 K for  $-1 \leq T_U \leq 1$  K.)

#### REFERENCES

- [1] S. H. Yueh, "Estimates of Faraday rotation with passive microwave polarimetry for microwave remote sensing of earth surfaces," *IEEE Trans. Geosci. Rem. Sens.*, vol. 38, no. 5, pp. 2434–2438, Sep 2000.
- [2] F. T. Ulaby, R. K. Moore, and A. K. Fung, *Microwave Remote Sensing: Active and Passive*. Artech House, 1986, vol. 2, ch. 7, pp. 478–488.
- [3] A. Papoulis, *Probability, Random Variables, and Stochastic Processes*, 3rd ed. New York: McGraw-Hill, 1991, exercise 6-16.
- [4] K. S. Miller, *Multidimensional Gaussian Distributions*, ser. SIAM Series in Applied Mathematics. New York: Wiley, 1964, p. 28, 72.

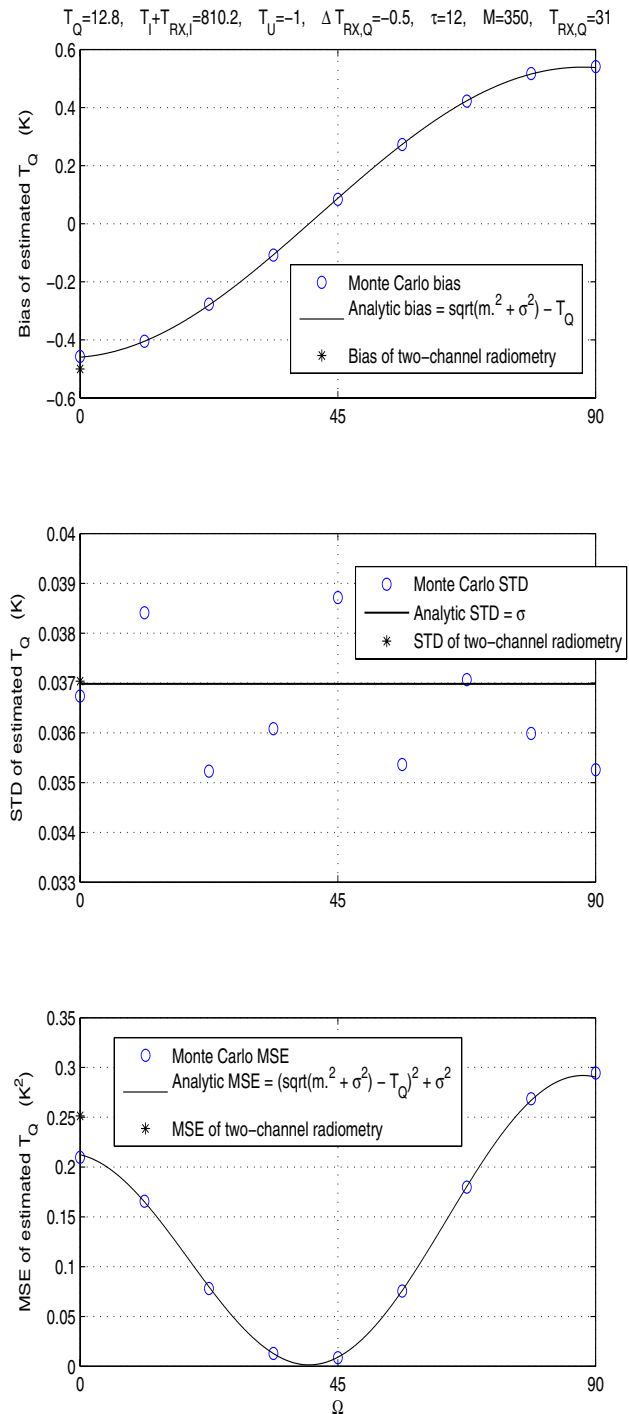


Fig. 1. Bias (top), STD (center), and MSE (bottom) of the estimated second Stokes parameter,  $\hat{T}_Q$ , as a function of  $\Omega$ , with typical Aquarius parameters (sea,  $\tau = 12$  s) and  $\theta = 23.3^\circ$ .

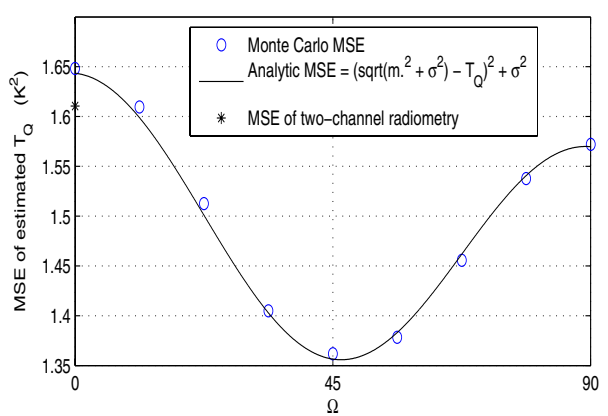
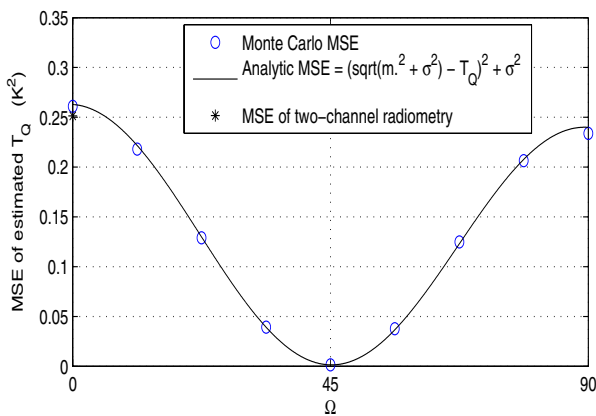
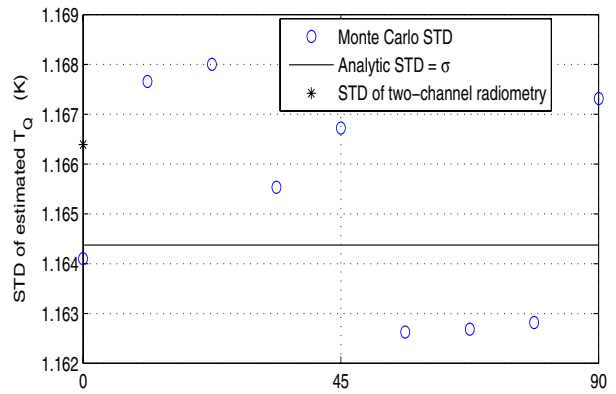
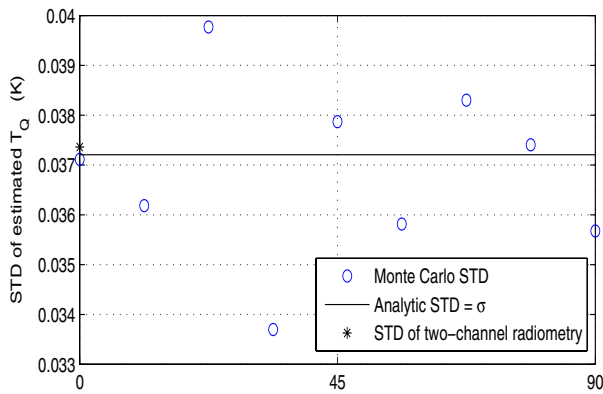
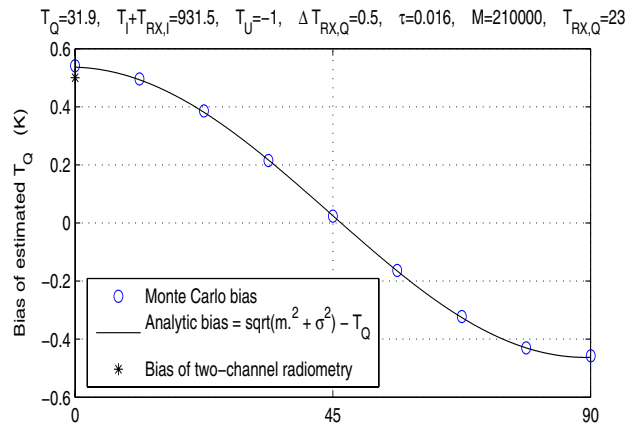
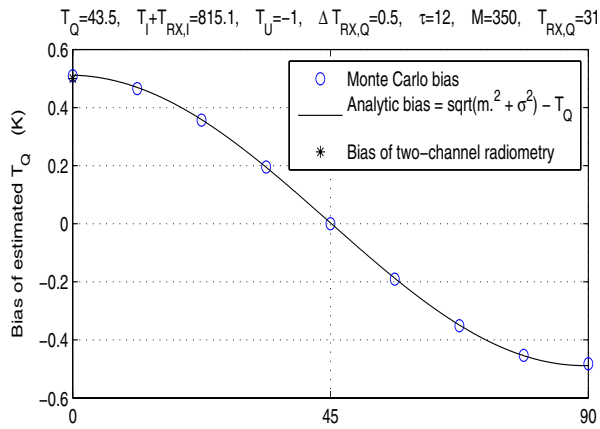


Fig. 2. Bias (top), STD (center), and MSE (bottom) of the estimated second Stokes parameter,  $\hat{T}_Q$ , as a function of  $\Omega$ , with typical Aquarius parameters (sea,  $\tau = 12$  s) and  $\theta = 41.7^\circ$ ).

Fig. 3. Bias (top), STD (center), and MSE (bottom) of the estimated second Stokes parameter,  $\hat{T}_Q$ , as a function of  $\Omega$ , with parameters typical of those proposed for soil moisture sensing at L-band (land,  $\tau = 0.016$  s,  $\theta = 41.7^\circ$ ).